



# Numerical Simulation of Coupled Heat and Mass Transfer for Airfoil Ice Protection Systems

Guilherme Araujo Lima da Silva, Daniel Ribeiro de Barros, Caio Fuzaro Rafael, Diogo Mendes Pio, Hamid Hefazi, and Marcos de Mattos Pimenta

## Contents

Introduction .....	3
Overview of Numerical Models for Ice Protection Simulation .....	4
Anti-ice Thermal Model .....	9
Runback Water Hydrodynamics Model .....	13
Water Film Model .....	13
Film Breakdown Criterion .....	13
Water Rivulets Model .....	15
Contact Angle .....	20
Momentum and Thermal Boundary-Layer Models .....	20
Kays and Crawford Momentum Boundary Layer in Integral Form .....	21
Walz and Head Momentum Boundary Layer in Integral Form .....	22
Convective Heat Transfer at Stagnation Point .....	24
Isothermal Thermal Boundary Layer in Integral Form .....	24
Non-Isothermal Thermal Boundary Layer in Integral Form .....	24
Thermal Boundary Layer by Superposition .....	25
Laminar-Turbulent Transition .....	27
Momentum and Thermal Boundary Layer in Differential Form .....	30

---

G. Araujo Lima da Silva (✉)  
Aerothermal Solutions LLC, Miami, FL, USA  
e-mail: [gasilva@aerothermal.co](mailto:gasilva@aerothermal.co)

D. R. de Barros · C. F. Rafael · D. M. Pio  
Aerothermal Solutions, Sao Paulo, Brazil  
e-mail: [daniel@aerothermalsolutions.co](mailto:daniel@aerothermalsolutions.co); [caio@aerothermalsolutions.co](mailto:caio@aerothermalsolutions.co);  
[dpio@aerothermalsolutions.co](mailto:dpio@aerothermalsolutions.co)

H. Hefazi  
State University of New York Korea, Songdo, South Korea  
e-mail: [hamid.hefazi@sunykorea.ac.kr](mailto:hamid.hefazi@sunykorea.ac.kr)

M. d. M. Pimenta  
University of Sao Paulo, Sao Paulo, Brazil  
e-mail: [mpimenta@usp.br](mailto:mpimenta@usp.br)

Numerical Code Description .....	31
Solvers .....	31
Numerical Implementation .....	32
Modeling Levels .....	32
Physics Test Cases .....	35
Flat Plate Tests .....	35
ERCOFTAC Tests .....	35
Airfoil MBB-V2 .....	37
NACA Airfoil Anti-ice Tests .....	39
Anti-Ice Reference Cases .....	39
Physics Validation .....	43
Flat Plate Cases .....	43
ERCOFTAC Cases .....	45
Airfoil MBB-V2 Cases .....	49
NACA Airfoil Anti-ice .....	55
Results from Anti-Ice Simulations .....	61
Original Model with Reynolds-Kays-Kline (RKK) Transition .....	61
Original + Rivulets with RKK Transition .....	61
Original + RKK Transition Vs. Isothermal + Abrupt Transition, both Considering Rivulets .....	61
Original + Rivulets Vs. Superposition + Rivulets with RKK Transition, both Considering Rivulets .....	75
Original + Rivulets Vs. BLP2C Code, both with Abu-Ghannan and Shaw (AGS) Transition Prediction and Intermittency .....	75
Conclusions .....	81
References .....	89

## Abstract

The design of ice thermal protection systems is multidisciplinary and highly integrated with that of other aircraft systems and aircraft aerodynamics, thus requiring knowledge of atmospheric conditions, numerical simulation methods, and testing procedures for aircraft to be certified under national airworthiness regulations. Using simulations in the certification process may reduce the required icing tunnel and flight tests, provided that the system's thermal behavior is accurate. Simulations can anticipate system thermal performance by predicting surface temperatures, runback water flow, and runback freezing rates. The results demonstrate compliance with regulations and are validated by tests in the certification phase of the aircraft. A thermal analysis code applies the first law of thermodynamics and the water continuity equations to the airfoil exposed to icing conditions in a steady-state regime. In addition to the effects of phase change by evaporation, freezing, and melting, the code considers the impact of the streamwise temperature gradient, water hydrodynamics, and laminar-turbulent transition. Correlations predict both the onset and length of the laminar-turbulent transition. The runback water flow is assumed to follow two regimes: film and rivulets. Within the impingement limits, runback water runs as a film and flows downstream as rivulets. The present chapter also uses two other procedures: (1) the superposition method and (2) a 2D boundary-layer differential code by Reynolds Averaged Navier Stokes. Results from non-isothermal and isothermal superposition and differential boundary layers were compared with experimental data from the NASA icing tunnel, which were used to validate the proposed code.

---

**Keywords**

Ice protection · Boundary layer · Transition · Convective heat transfer ·  
Evaporative cooling · Water rivulets · Water film · Non-isothermal heat transfer

---

**Introduction**

Ice accretion on airframes can significantly reduce the operational safety margins of aircraft and, consequently, hinder aircraft compliance with applicable aeronautical regulations. Therefore, the impact of ice accretion on systems functions and aircraft aerodynamics must be analyzed in earlier stages of aircraft development.

This early analysis makes it possible to define which systems and aircraft surfaces will potentially require ice protection. Moreover, to start trade-off studies for ice protection strategies balancing the energy necessary for ice protection, proper operation of other aircraft systems, aircraft performance, flight qualities, type of aircraft operation, and compliance and engine certification requirements.

Some specific surfaces include wing and stabilizer leading edges, engine and Auxiliary Power Units (APU), air inlets, flight deck transparencies, ventilation air inlets and outlets, air data sensors, fairings, and antennae.

Ice accretion on aircraft wings and stabilizers may cause aerodynamic performance degradation, aircraft weight increase, and control and maneuver difficulties, leading to a reduction in operational safety margins when the aircraft is flying through clouds of supercooled water droplets in a metastable state. Therefore, ice accretion on some aerodynamic surfaces will occur if they are not adequately protected. Civilian and military aircraft have ice protection systems to protect the airfoils and guarantee safe flight in icing conditions. Depending on how these systems operate, they are classified as de-icing or anti-ice.

An anti-ice system prevents any ice accretion on airfoils and continuously operates while the aircraft flies under icing conditions.

An electrothermal anti-ice system, for instance, consists of a set of electrical heaters installed in the areas exposed to icing. Anti-ice systems can operate under three regimes:

1. **Fully evaporative:** impinging water droplets are vaporized close to the impingement region.
2. **Evaporative:** runback water flows over the airfoil leading edge and evaporates in a position upstream of the end of the protected area.
3. **Running wet:** runback flows downstream at the end of the protected area.

Consequently, in the running wet regime, if the runback water flows to regions downstream of the thermally protected zone, that water will freeze and form runback ice. Depending on residual ice height, shape, and roughness, significant degradation of airfoil aerodynamic characteristics may occur.

With an activated thermal anti-ice system, water droplets impinge and form a thin water film at the stagnation area. Then the runback water flows to downstream regions driven by pressure and shear forces applied by the external flow around the airfoil. Due to evaporation, external flow pressure gradient, shear stress, or heating effects, runback water thickness varies streamwise. The water film may break up and form rivulets if a critical thickness is reached. A decrease in the wetted area marks the transition from film to rivulets because dry patches start to grow between rivulets.

In summary, rivulet flow affects the effectiveness of anti-ice systems because it reduces the heat transfer areas between the water and the airfoil surface and reduces the area of heat and mass transfer between the water and the external flow. For the same film spanwise width, solid-liquid and liquid-vapor contact areas are smaller in a rivulet flow than in a liquid-water film flow regime. Consequently, rivulet formation increases the demand for heating and may cause the water to flow downstream to an unprotected region.

An adequate thermal anti-ice numerical code is essential for conceiving a system, defining its architecture and size, and for system development. In addition, during the certification phase, a validated code helps support the definition of a critical case matrix and test campaign planning.

Electro-thermal anti-ice systems have been the focus of attention lately due to the advent of electric airplanes, where an electrical generator provides all the power. In this electrical vehicle case, the electro-thermal type of system is more common. In this kind of system, the ice accretes and melts cyclically. Therefore, the system is never operated in a steady state regime like anti-icing.

---

## Overview of Numerical Models for Ice Protection Simulation

The classic icing codes LEWICE (Macarthur et al. 1982; Ruff and Berkowitz 1990), TRAJJICE2 (Cansdale and Gent 1983; Gent 1990), and ONERA2D (Guffond and Brunet 1988) estimate ice shapes over nonprotected airfoil surfaces. A comprehensive review of mathematical models and comparing these codes' prediction capabilities were published by Wright, Gent, and Guffond (Wright et al. 1997). The main modules of these classic icing codes are:

1. **Flow field**, which solves the flow around an airfoil.
2. **Droplets trajectories**, which calculate droplets trajectories and the local collection efficiency; and
3. **Thermal balance** estimates ice growth and its two-dimensional shape by applying the first law of thermodynamics to water and adiabatic solid surface around the airfoil leading edge.

Most anti-ice numerical codes use the first and second modules but replace the third one with another that considers anti-ice heat flux distribution to calculate surface temperatures and runback mass flow rate.

At the British Royal Aircraft Establishment, Cansdale and Gent (1983) implemented one of the pioneering works regarding thermal balance around non-heated airfoils under icing conditions by extending Messinger's (Messinger 1953) mathematical model to compressible flow and water vapor local concentration. Gent (1990) implemented the numerical code TRAJICE2, predicting two-dimensional ice shapes on airfoils. The author approximated the flow over the airfoil leading edge as similar to one over the frontal part of a cylinder and, by scaling experimental results of heat transfer around rough cylinders, developed an empirical expression to evaluate the convection heat transfer coefficient on airfoil surfaces. The author implemented a boundary layer integral analysis to assess laminar and turbulent heat transfer coefficients over a near isothermal surface without mass transfer effects. The laminar to turbulent transition is assumed to occur when the critical Reynolds number based on roughness height is 600. As with other classic icing codes, the heat transfer prediction is only valid for thin ice accretions, i.e., at the beginning of the accretion process, in the absence of flow separation (Gent et al. 2000).

Gent et al. (2003) developed a rotorcraft airfoil de-icing code that evaluates heat transfer coefficient distribution with the same procedure adopted in TRAJICE2. However, the authors concluded that convective heat transfer coefficient evaluation during de-icing operations should be improved in future research.

Makkonnen (1985) proposed a calculation procedure for laminar, transitional, and turbulent heat transfer between an air stream with droplets and a rough surface of a roughened cylinder. The author used a heat transfer coefficient to predict icing in wires of electrical power transmission lines. The heat transfer coefficient around the cylinder surface was evaluated through a boundary layer integral analysis based on the work of Kays and Crawford (Kays and Crawford 1993). He implemented a laminar boundary layer conduction thickness with Smith and Spalding's (Smith and Spalding 1958) and a turbulent Stanton number expression, which requires a boundary layer analysis, such as the one estimated experimentally by Pimenta et al. (Pimenta et al. 1975). The laminar and the turbulent convective heat transfer coefficients were evaluated through an analogy between momentum and heat transfer that considers a flow over a near isothermal surface without mass transfer. Additionally, Makkonnen (Makkonnen 1985) adopted an abrupt laminar to turbulent flow transition and considered momentum thickness continuous at the transition point, i.e.,  $\delta_{2,\text{lam}} = \delta_{2,\text{turb}}$ .

Wade (1986) and Downs and James (1988) developed a numerical code to simulate a hot air engine inlet anti-ice system. The authors used semi-empirical correlations to calculate the convection heat transfer coefficients in two regions of the engine inlet:

1. Between the impinging hot air jets from the piccolo tube and the inner nacelle lip leading edge.
2. Between the free streamflow and the exposed surface of the nacelle leading edge.

Downs and James (1988) modeled the external flow field as a combination of a flow around the frontal part of a cylinder and a flow along with two parallel flat plates. Therefore, the cylinder and flat plate correlations were forced to match to reduce the deviation between numerical results and test data. To improve the convective heat transfer evaluation and obtain solid surface temperature results closer to test data, Riley (1991) used a CFD numerical tool to solve the flow field and estimate the heat transfer on nacelle lip external surfaces exposed to droplet impingement and on internal surfaces subject to engine bleed air heating.

Henry (1989) developed a numerical code to predict parameters of de-icing systems operation: he modified ONERA2D (Guffond and Brunet 1988) by introducing a different thermal balance procedure for de-icing simulations. Later (Henry 1992) applied a finite-difference boundary layer solver to evaluate laminar and turbulent heat transfer coefficients over airfoil non-isothermal surfaces coupled with a transient two-dimensional water freezing front based on an enthalpy method (Raw and Schneider 1985).

Al-Khalil (1991) developed a mathematical model that considers rivulets' effects on thermal balance. In a later work, he and his colleagues (Al-Khalil et al. 2001) implemented the ANTICE numerical code to predict the parameters of a thermal anti-ice system operation. This code uses the flow solver and droplet trajectory routines from the LEWICE code (Wright 1995, 1999). Al-Khalil et al. (2001) modified the thermal balance to simulate anti-ice operation by considering the distribution of airfoil surface heat flux and by using a complete runback model with liquid water film breaking down into rivulets.

Morency et al. (1999a, b) implemented a numerical code for anti-ice simulation. The results were validated with experimental data from Al-Khalil et al. (Al-Khalil et al. 2001). Morency et al. published results regarding two versions of the main code:

1. **CANICE A**, which uses an experimental overall heat transfer coefficient.
2. **CANICE B** considers the effects of streamwise airfoil surface temperature gradients when performing the thermal turbulent boundary layer integral analysis.

Neither the model of laminar to turbulent flow transition nor the procedure to define heat transfer coefficient described the turbulent boundary layer virtual origin. Morency et al. (1999a, b) published the results of **CANICE FD**, which uses a finite difference to calculate momentum, heat, and mass transfer. The adopted procedure considered the laminar and turbulent boundary layer and the transition region. Additionally, it used the Cebeci–Smith mixing length turbulence model for eddy viscosity, which includes an intermittency function for the transition between laminar and turbulent flow regimes (Cebeci and Bradshaw 1984).

Silva and Silvaes (2002) described the development of a thermal anti-ice mathematical model in detail, and it was summarized in Silva's bibliography research, results, conclusions, and contributions (Silva, April 2002).

In two different works, Silva, Silvaes, and Zerbini (Silva et al. 2003, 2005) briefly described the above-mentioned mathematical model, presenting some numerical code

results and comparing them with experimental data and with other codes' results for an anti-ice system operating in evaporative and running wet regimes. Their mathematical model for anti-ice system simulation, detailed, analyzed, and described herein, applies the first law of thermodynamics to liquid water flow and solid airfoil surface, and the conservation of mass and momentum to liquid water flow.

In the first stages of mathematical model development, Silva (Silva, April 2002) tried to use the ONERA2D boundary layer evaluation procedure, which adopts the Makkonnen model (Makkonnen 1985). However, the heat transfer coefficient in the turbulent region was overestimated. Much like other classic icing codes, ONERA2D evaluates convection heat transfer over fully rough surfaces. Makkonnen's (1985) procedure assumes an abrupt laminar to turbulent transition triggered by roughness. It neglects the effects of streamwise temperature gradient and the coupling between evaporation and thermal boundary layer growth. Therefore, Silva et al. (2003, 2005) implemented a numerical code to evaluate the integral equations of momentum and thermal boundary layer considering a non-isothermal airfoil surface with evaporation in laminar, transition, and turbulent flow regimes.

Silva et al. (2006) later adopted the minimum total energy (MTE) , which was introduced by Hobler (Hobler 1965) and developed by Mikielewicz and Moszynski (Mikielewicz and Moszynski 1975, 1976) because it:

1. Considers contact angle effects.
2. Estimates critical film height, wetness factor, and rivulet radius.
3. Presents acceptable deviations between predictions and several experimental data sets.

Mikielewicz and Moszynski (1975, 1976) considered a film flow followed by the flow of a semi-cylindric-shaped rivulet. They considered that both had a one-dimensional velocity distribution and were driven by either gravity or shear flow. Mechanical total energy and mass were conserved at film breakdown in the transition from film to rivulet flow, and the most stable rivulet distribution was found by minimizing total energy.

Three works by Al-Khalil (1991), Al-Khalil et al. (1993, 1994) proposed a rivulet model for application in airfoil thermal anti-ice simulations. The authors adopted film break-up based on minimum total energy criteria (Mikielewicz and Moszynski 1975, 1976). Still, they considered two-dimensional velocity distribution within a rectangular-shaped rivulet using numerical and interpolation procedures similar to that of previous works (Allen and Biggin 1974; Bentwich et al. 1976).

Recent developments in film break-up and rivulet formation consider the MTE criteria and a two-dimensional velocity field within the cross-section but calculate rivulet shape (Saber and El-Genk 2004; El-Genk and Saber 2001, 2002) instead of assuming it is cylindrical or rectangular. These developments showed a much smaller deviation between numerical results and experimental data than in previous works.

Gosset (2017) addressed different methods to predict the breakup of a runback water film into rivulets. The Minimum Total Energy (MTE) criterion was first

applied to a sheared film on a NACA profile and then confronted with experimental data. The author developed both experimental and analytical or computational studies. After this, the film solver in the CFD code OpenFoam was used to compute the breakup of a falling film on an inclined plane. OpenFoam simulations agreed more with experimental data for film breakup than did the MTE criterion because the former does not use all the simplified assumptions of MTE, such as shape, rectilinear path, and constant spacing, among others.

Gutiérrez et al. (2021) presented a numerical model for the operation of an electro-thermal Ice Protection System (IPS) for an airfoil. The results obtained were pretty in agreement with experimental data. Their work compared results with the integral boundary layer developed by Silva et al. (Silva et al. 2009), which did not work well with fully automatic transition prediction from the Abu-Ghannan and Shaw (AGS) model. The authors did not compare differential results with the AGS transition used by Silva et al. (2009), which was much more compatible with experimental data.

In 2002, Tran et al. (2002) successfully validated FENSAP-ICE results against experimental data. Their droplet impingement module accurately predicted high catch regions, which may require anti-icing protection. The ice accretion module was used to compute ice shapes on unprotected surfaces, and the heat load module optimized the power output needed to protect critical surfaces.

Domingos et al. (2007) described part of the engine inlet anti-ice system development based on numerical simulation and icing wind tunnel tests. Several critical cases were selected from Appendix C. The selected configurations and conditions were tested in an Icing Wind Tunnel, where piccolo flow parameters were optimized, and data were collected to provide a basis for validating the numerical tools. Although not cited, the boundary layer code used was the one developed by Silva et al. (Silva et al. 2003).

Elangovan and Olseny (2008) implemented a transient simulation of a de-icing system of an airfoil by using a finite difference scheme to solve the conduction heat transfer on the solid sandwich material. The authors considered the conduction, external convection, and runback water flow without rivulets. External codes or correlations mainly provide the heat transfer coefficient.

Silva et al. (2009) implemented an anti-ice code that uses a modified differential boundary code, a fully automatic transition prediction, and a water runback hydrodynamics model with film and rivulets. Results were very encouraging and show that a differential boundary layer adequately captures flow history's effects.

de Souza et al. (2016) developed theoretical–experimental studies at COPPE/UFRJ on conjugated heat transfer problems associated with the transient thermal behavior of heated aeronautical Pitot tubes. Their work included flight test validation with the military aircraft A4 Skyhawk (Brazilian Navy) and wind tunnel runs (NIDF/COPPE/UFRJ). The convective heat transfer problem in the external fluid was solved using boundary layer equations for compressible flow and applying the transformation of the Illingworth variable considering a locally similar flow. Nonlinear partial differential equations were solved using the Generalized Integral Transform Technique (GITT). In addition, an entirely conjugated problem model was proposed,



including both dynamic and thermal boundary layer equations for laminar, transitional, and turbulent flow coupled with heat conduction.

## Anti-ice Thermal Model

This model is based on the works of Silva (Silva, April 2002) and Silva, Silvaes and Zerbini (Silva et al. 2003). It was modified to include rivulet effects (Silva et al. 2006).

Figure 1 shows the coordinate system and the five domains used in the present mathematical model, namely:

1. Freestream flow.
2. Gaseous flow.
3. Momentum or thermal boundary layers.
4. Water flow; and
5. Solid surface.

The mathematical model may be organized and simplified using the domain division strategy above. The first law of thermodynamics applied to a solid surface (domain 5) results in:

$$\begin{aligned} \frac{d}{ds} \left( k_{wall} \cdot \frac{dT_{wall}}{ds} \right) - F \cdot h_{water} \cdot (T_{wall} - T_{water}) + \dot{q}''_{anti} + (1 - F) \\ \cdot [-h_{air} \cdot (T_{wall} - T_{rec})] \\ = 0 \end{aligned} \quad (1)$$

Where:

$$T_{water} = (T_{in} - T_{out})/2 \quad (2)$$

The First Law of Thermodynamics applied to water in both film and rivulet flow patterns is expressed as:

$$\begin{aligned} \xi \cdot F \cdot A \cdot h_{air} \cdot (T_{rec} - T_{water}) + F \cdot A \cdot h_{water} \cdot (T_{wall} - T_{water}) + \dot{m}_{in} \cdot c_{p,water} \cdot (T_{in} - T_{ref}) \\ - \dot{m}_{out} \cdot c_{p,water} \cdot (T_{out} - T_{ref}) + A \cdot \dot{m}_{imp} \cdot \left[ c_{p,water} \cdot (T_d - T_{ref}) + \frac{V_d^2}{2} \right] \\ + \xi \cdot F \cdot \dot{m}_{evap} \cdot [i_{lv} - c_{p,water} \cdot (T_{out} - T_{ref})] = 0 \end{aligned} \quad (3)$$

By definition, the overall wetness factor is given by:

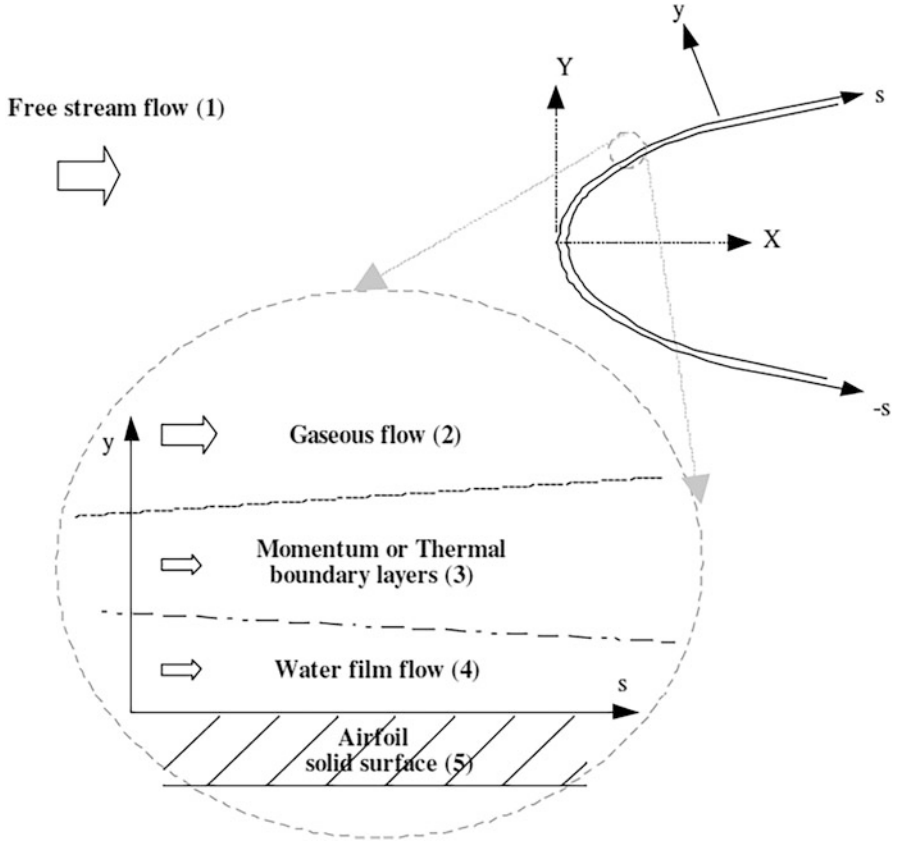


**Fig. 1** Domains of the mathematical model

$$F = \frac{A_{wet}}{A_{total}} \quad (4)$$

$$A_{total} = A_{wet} + A_{dry} \quad (5)$$

The convection heat transfer coefficient between a water film (4) and a solid surface (3) is calculated by the Colburn analogy between momentum and heat transfer:

$$h_{water} = \rho_{water} \cdot \nu_f(s, \delta_f) \cdot c_{p,water} \cdot 0.5 \cdot C_f \cdot Pr_{water}^{-2/3} \quad (6)$$

Water thermodynamics properties are evaluated for low-speed flows according to Eckert's work (Eckert 1955) at the temperature:

$$\bar{T}_{water} = T_{wall} + 0.5 \cdot (T_{water} - T_{wall}) \quad (7)$$